Structural Analysis of the Central Sumatra Basin Using Geological Mapping and Landsat 8 Oli/Tirs C2 L1 Data

Kausarian, Husnul
Engineering Geological Program, Faculty of Engineering, Universitas Islam Riau

Redyafry, Lady
Engineering Geological Program, Faculty of Engineering, Universitas Islam Riau

Josaphat Tetuko Sri Sumantyo
Center for Environmental Remote Sensing, Chiba University

Suryadi, Adi
Engineering Geological Program, Faculty of Engineering, Universitas Islam Riau

他

https://doi.org/10.5109/6792830

出版情報：Evergreen. 10 (2), pp.792-804, 2023-06. 九州大学グリーンテクノロジー研究教育センター
バージョン：

Structural Analysis of the Central Sumatra Basin Using Geological Mapping and Landsat 8 Oli/Tirs C2 L1 Data

Husnul Kausarian[1,*], Lady Redyafry[1,2], Josaphat Tetuko Sri Sumantyo[3,4], Adi Suryadi[1], Muhammad Zainuddin Lubis[5]

[1]Engineering Geological Program, Faculty of Engineering, Universitas Islam Riau, Indonesia

[2]Analyst 2 Core Section, Duri Laboratory, PT. Sucifindo, Indonesia

[3]Center for Environmental Remote Sensing, Chiba University, Japan

[4]Department of Electrical Engineering, Faculty of Engineering, Universitas Sebelas Maret, Indonesia

[5]Department of Geomatics Engineering, Politeknik Negeri Batam. Batam, Indonesia

*Author to whom correspondence should be addressed:
E-mail: husnulkausarian@eng.uir.ac.id

(Received December 4, 2022; Revised May 2, 2023; accepted May 24, 2023).

Abstract: The Great Sumatran Fault is the main fault on the island of Sumatra, which stretches throughout the island, and one of its products is Central Sumatra Basin. The research area is an area that developed from the Central Sumatra Basin at the time of its formation, and this research area is in Pulau Padang Village. This study focuses on the geological and structural developments due to the Central Sumatra Basin. Central Sumatra Basin is the main producer of oil and gas in Indonesia. River straightness patterns, lithological offsets, and others can indicate the fault structure. Based on satellite image data and digital elevation models, there are indications of fault structures appearing in the research area and its surroundings. This can be seen from the straightness of the Bukit Mudoh's river. This anomaly is visible in the river's flow pattern, which shows a significant change in the upstream area, which is in the form of a trellis, then changes instantly to a straight line. Based on the appearance of the Landsat 8 OLI/TIRS C2 L1 satellite image, there is a hill offset that shifts with the movement of the fault. This is also supported by data supporting the tectonic framework of the Central Sumatran Basin, which indicates a compression phase during the Middle Oligocene to Middle Miocene with a North-South direction of stress and reactivation in the Pliocene–Pleistocene.

Keywords: Environmental Setting; Geological Structure; Landsat 8; Great Sumatran Fault; Central Sumatra Basin

1. Introduction

Sumatra Island is one of the large islands in Indonesia, which contains the Bukit Barisan Mountains, a mountain range that stretches 1,650 km of Sumatra[1)-5)]. The Bukit Barisan was formed due to a fault structure in Sumatra that developed from the Miocene to the Pliocene - Pleistocene period known as The Great Sumatran Fault[6)-10)]. The current tectonics in Central Sumatra, especially in the Riau and surrounding areas, is strongly influenced by the subduction of the Indo-Australian plate with the Eurasian plate. With an average range of 60 mm/year[11)-14)], plate movements continue to occur. This can trigger movement in a small part of Riau Province, which is touched by the Bukit Barisan zone, such as in the research location. The research area is Pulau Padang Village, Singingi District, Kuantan Singingi Regency, Riau Province, Indonesia. Geographically, the research area is located at coordinates 00º24'00" - 00º27'23"S and 101º16'56" - 101º19'25"E (Fig. 1).

The analysis of the geological structure in the research area is fascinating because it can produce valuable information for further research regarding the detailed conditions of the geological structure that developed due to the formation of the Great Sumatran Fault that stretches along the island of Sumatra. With this geological structure analysis, the pattern formed because of the formation of the Great Sumatran Fault can be determined. One of the most valuable methods to see the formation of geological structures in this Great Sumatran Fault area is to use analysis of Landsat 8 OLI / TIRS C2 L1 satellite imagery[15)-16)], which displays geological conditions in the form of results such as geological maps, geological structure maps, geomorphological maps, and maps of -

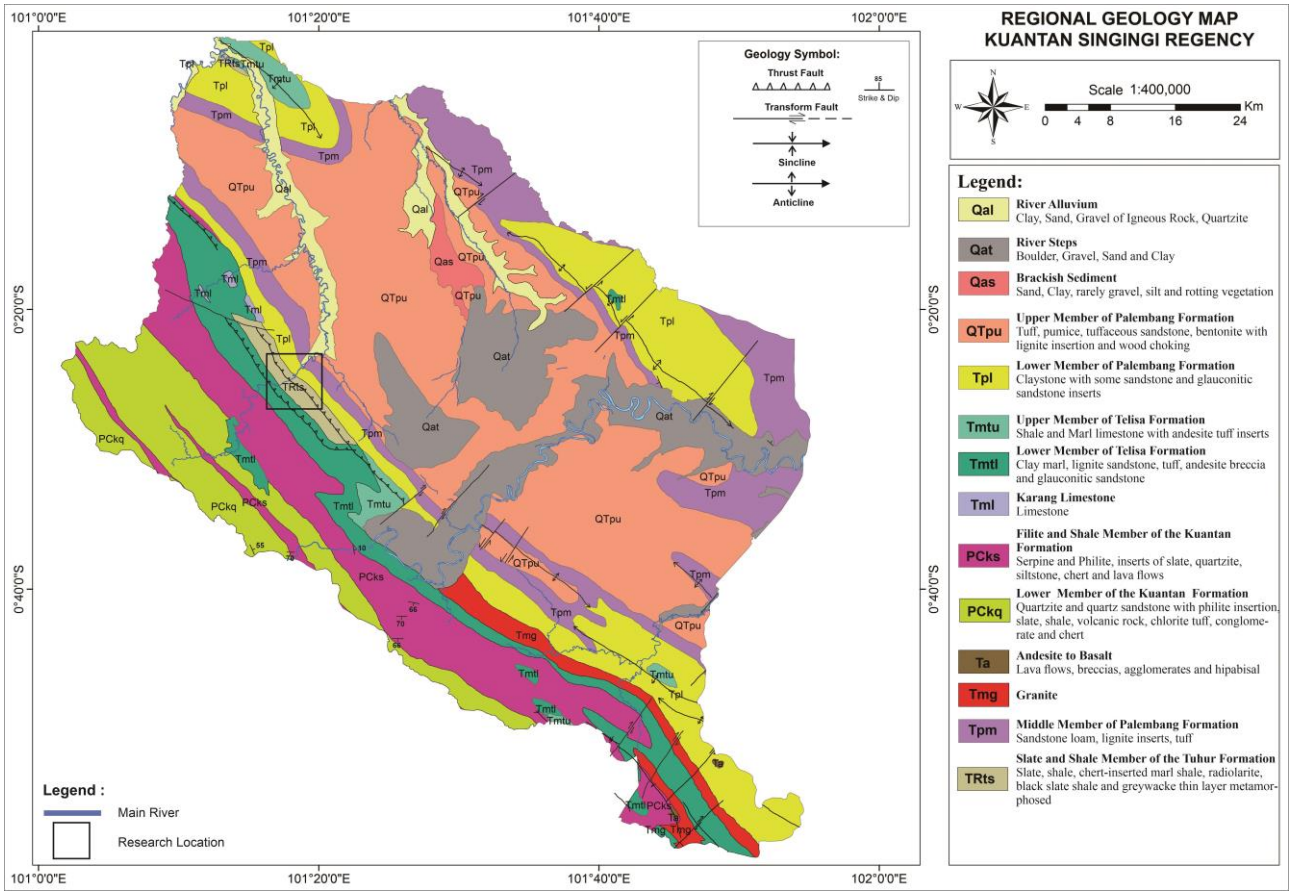

Fig 1: Corrected Geological Map of the Research Area from the Field Observation (modified from Silitonga and Kastowo, 1975).

river flow patterns (stream order) due to structures that develop in the research area.

This research aims to see indications of the appearance of fault structures using visual satellite image data located in the Pulau Padang Village and its surroundings. Field geological observations are also carried out to record geological condition data in the form of lithology types, geological structures that develop, flow patterns and geological structures that are currently developing at the research site so that they can integrate the analysis of geological data obtained from visual data from Landsat images combined with field data.

In this study, the objective sought to improve our understanding of the structural framework of the Central Sumatra Basin. The Central Sumatra Basin is a region of great interest to the oil and gas industry, and a better understanding of its geological and structural characteristics could aid in future exploration efforts. The researchers aimed to identify and map the fault structures in the Pulau Padang Village area, which is located within the Central Sumatra Basin, using a combination of remote sensing data and field validation.

To achieve this objective, satellite image data and digital elevation models have been used to identify river straightness patterns, lithological offsets, and hill offsets, which are indicators of fault structures. This study also conducted geological mapping and field validation to support this study. Ultimately, this study hoped would provide new insights into the geological history of the Central Sumatra Basin and help to guide future exploration efforts in the region for exploring more oil and gas in this basin.

2. Geological background and methods

2.1 Geological background

The research location is part of the Central Sumatra Basin, a basin formed behind the magmatic arc during the Early Tertiary (Eocene - Oligocene) as a series of half-graben structures separated by a block horst because of the subduction process of the Indian Ocean plate infiltrating under the plate. Central Sumatra Basin is the main producer of oil and gas in Indonesia and the Asian continent[17)-21)]. This basin is an asymmetrical shape that leads to the Northwest - Southeast. The deepest part is in the southwest and slopes towards the northeast.

The Central Sumatra Basin is bounded to the west and southwest by Bukit Barisan, to the east by Peninsular Malaysia, to the north by the Asahan Arc, to the southeast by the Tigapuluh highlands and to the northeast by the Sunda Kraton. At the same time, the southern boundary has yet to be well known[22)-25)]. Furthermore, this half-graben formation is filled by non-marine clastic sediments and lacustrine from the bund group in some parts of the

deep graben. Central Sumatra has experienced several phases of complex deformation, which has directly affected the source rock distribution, the development and formation of reservoirs and their geological structure. The Central Sumatra Basin has undergone several phases of complex deformation. This has directly affected the source rock's distribution, the reservoir's development and formation and its geological structure.

The geology of Pulau Padang Village shows the distribution of rocks consisting of the Tuhur Formation, the Lower Member of the Palembang Formation, and the Lower Member of the Telisa Formation (Fig. 1). The Tuhur Formation consists of slate lithology, shale members and limestone members. The age of this formation is Triassic. All these rocks were then intruded on by Lassi Granite which was 200 million years old[26)-29)]. The Lower Member of the Palembang Formation[30), 31)] occurred during the shrinking of seawater and consisted of Claystone with some sandstone and glauconitic sandstone inserts. The Lower Members of the Telisa Formation[32), 33), 34)] were deposited during maximum transgression and developed well throughout the Central Sumatra Basin. This formation consists of Clay, lignite sandstone, tuff, andesite breccia and glauconitic sandstone.

2.2 Methods

The literature study was conducted to study and collect related previous research results as a theoretical basis for the problems to be reviewed, such as regional geology of the research area, remote sensing, satellite image specifications and other supporting references. The data collection included data from Landsat 8 satellite imagery[35)] for the Pulau Padang Research area, Geological Map data from Solok Sheet at a scale of 1:250,000, Indonesian Earth Map data at a scale of 1:25,000, and data from outcrop observations. Lithology, joint structure. Observation data of geological structures in the field is used to indicate the location of certain geological conditions in satellite imagery so that the lineament pattern at the observation location can be known. The lithological survey at the research area is in the form of a description of the geological conditions encountered, plotting the sample locations, and documentation of field conditions. The result is a record of geological observations of the research location.

The data used in this study consisted of Landsat 8 imagery on Path 127 and Row 60, the Indonesian topographical map, the Solok Sheet Geological Map, and field geological observation data using Garmin 64S GPS. The data retrieval technique using GPS Garmin 64S is the data taken at several coordinates of the observation location to get the geomorphological conditions, river flow patterns (stream order), geological structures, slopes, and other geological-related information. Observation data of geological structures in the field is used to indicate the location of certain geological conditions in satellite imagery so that the lineament pattern at the observation location can be known.

In Landsat 8 imagery, systematic geometry correction has been applied, but radiometric correction still needs to be done because the image data is in Digital Number (DN) format[36), 37)]. There are two types of output images produced in reflectant format, namely Top of Atmosphere (TOA) or reflectants captured by the sensor and Bottom of Atmosphere (BOA) or reflectants on objects that have been corrected by the atmosphere. Radiometric correction is a crucial step in processing Landsat 8 satellite imagery because Landsat 8 is at level 1T (terrain corrected), so the image does not need to be corrected geometrically. Radiometric correction is divided into two stages: radiometric calibration and atmospheric correction. The radiometric calibration process in this study used VISAT 5.0 software with several steps; Change the Digital Number (DN) value to radians ($L\lambda$), Change the Digital Number (DN) value to reflectance ($\rho\lambda$), and change the reflectance value ($\rho\lambda$) to sun angle corrected reflectance ($\rho\lambda^*$).

Furthermore, to get the BOA reflectance value in the radian format image, an atmospheric correction process is carried out to obtain the correction value parameter. This process uses 6S Code to get the parameters xa, xb, and xc to produce a corrected BOA reflectance image from atmospheric influences. Furthermore, the image sharpening stage is carried out where the combination of Landsat-8 image channels uses a combination of channels 5, 6, and 7 in the arrangement of red, green, and blue channels (red, green, blue/RGB). Channels 5, 6, and 7 are infrared channels (Indrastomo et al., 2015). The band ratio used with the combination of Landsat 8 channels is red, green, and blue (red, green, blue/RGB), namely 4/2, 5/6, and 6/7 channels[38)-39)]. The combined image of this channel will produce a composite image with pseudocolor. This channel is sensitive to rock types of changes, so the rocks' distribution can be identified from this composite image.

Based on the combination of the results of Landsat 8 imagery and the recorded geological structure observations in the field, an interpretation of the lineament pattern in the study area is carried out. Image classification is used to obtain geological interpretation results and determine regional zones with certain geological conditions. The classified images are then combined with the vector map digitised by the RBI map to get maximum classification results[40)]. After cutting the classified images, the above map was converted into vector format using ArcGIS software, followed by a cartographic process to produce a map display of the Geological structure of Pulau Padang Village. The whole process of the methodologies used in this research can be seen in Fig. 2.

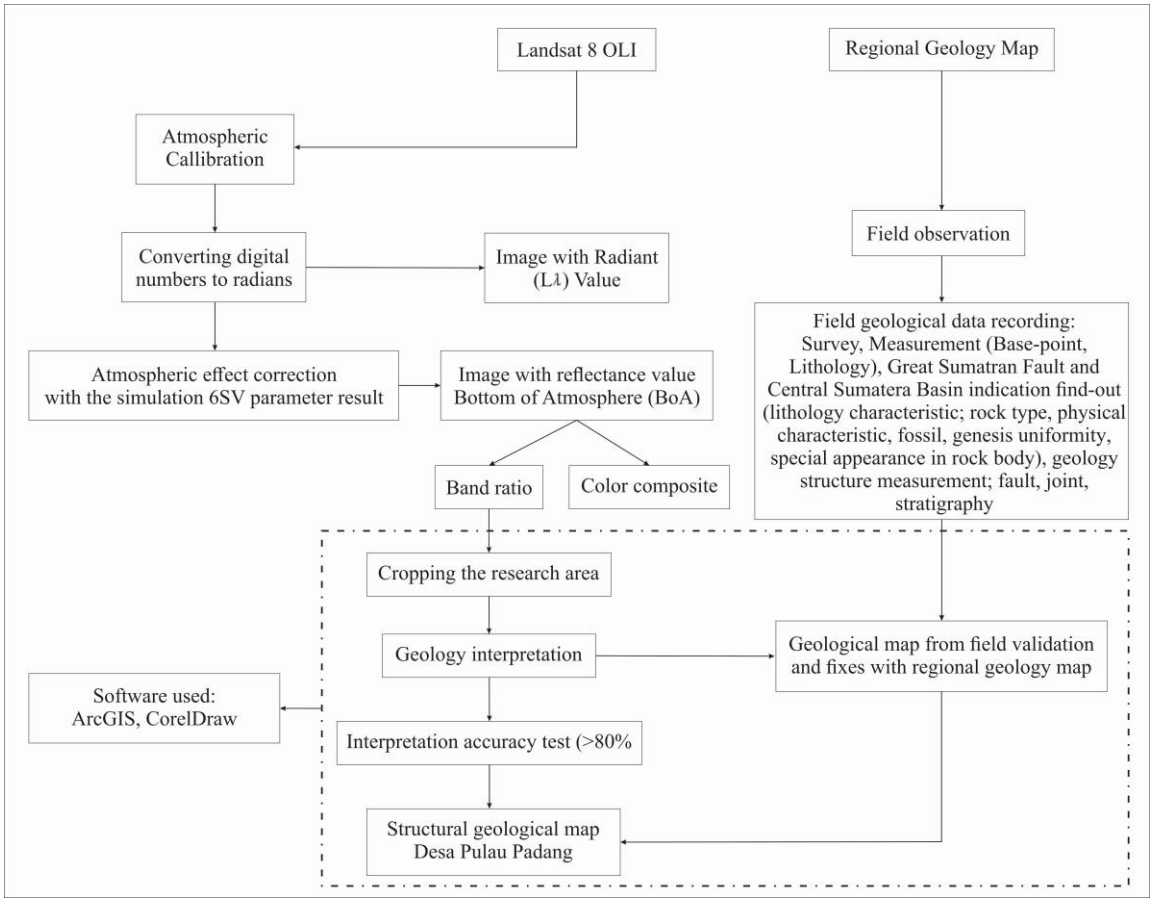

Fig. 2. Flowchart of methodology used in this research.

3. Result and discussion

3.1 Result

3.1.1 Image correction

Landsat 8 satellite imagery data used in this study is recorded from August 7, 2019 to September 3, 2022, with Level 1 Terrain (L1T). The data at this level results from processing Level 1 Radiometric (L1R) with the application of systematic geometry correction (Fig. 4a). This geometric correction process uses binding points or onboard position information for resampling the image so that the image is cartographically projected to WGS 1984. The processed data with the L1T level is also terrain corrected for relief displacement. Atmospheric correction reduces the object's reflectance from the total TOA radiance after normalising lighting conditions and eliminates atmospheric influences. In this study, Landsat 8 images were corrected for atmospheric effects using correction parameters from simulation results using the Second Simulation of a Satellite Signal in the Solar Spectrum - Vector (6SV). Atmospheric correction parameters processed by the 6SV method for Landsat 8 images in the study area are shown in Table 1. In this atmospheric correction, raw data from Landsat 8 is used to obtain the values of the sun's azimuth and zenith angles. To define the concentration of aerosols, a meteorological parameter is used in the form of horizontal visibility (in this image, visibility = 7.8 km), which is included in 6SV.

Table 1. Atmospheric correction parameter of 6SV.

No.	Channel	Parameter		
		xa	xb	xc
1.	Channel 2	0,00277	0,16280	0,20227
2.	Channel 3	0,00276	0,09446	0,15994
3.	Channel 4	0,00301	0,05925	0,12863
4.	Channel 5	0,00424	0,03010	0,08791
5.	Channel 6	0,01583	0,00875	0,03457
6.	Channel 7	0,05044	0,00319	0,01852

Aerosol thickness at 550 nm was then calculated based on the tropical atmospheric conditions and the Continental Model aerosol model. The results of the atmospheric correction with the 6S method are, from now on, referred to as SR-6SV. Then these three parameters are used to perform atmospheric correction on the radian format image to produce an image with a BOA reflectance.

3.1.2 Geological analysis from field observation

Based on validation in the field, the lithostratigraphic

units of the study area showed the stratigraphic order arranged from oldest to youngest: Schist Unit, Carbonate Calcite Claystone Unit, Fine Sandstone Unit, Medium Sandstone Unit, Conglomerate Sandstone Unit, Siltstone Unit, and Conglomerate Sand Unit Quarter (Fig. 3).

3.1.3 Geomorphology analysis

Geomorphology in the study area is grouped according to Van Zuidam's classification. The research area is grouped based on the relief, lithology, and genetic aspects and divided into three geomorphic subunits: Denudational of High Wavy Hills Geomorphological Sub-unit, Denudational of Remaining Hilly Landform Geomorphological Sub-Unit, Structural Landform (Horst) Very Steep Geomorphological Sub-Unit (see Fig. 3).

a. Denudational of high-wavy hills geomorphological sub-unit

This geomorphological unit (D.1) covers 30% of the entire research area, which occupies the West-Southwest part of the study area. The flow pattern in this geomorphological unit is sub-dendritic. Elevation 14-20º with an altitude of 112 to 200 mdpl, slope 13-25%, in the form of high undulating hilly land (Fig. 4). The developing structure is like a shear fault. The lithology that composes this geomorphological unit is carbonated claystone, carbonated calcite, fine sandstone to coarse sandstone, conglomerate sandstone and coal weathering remnants that act as fragments in very fine sandstone. Exogenous processes in the form of weathering due to erosion by water, rubber plantations, oil palm plantations, and wood refineries of the surrounding community.

b. Denudational of remaining hilly landform geomorphological sub-unit

This geomorphological unit (D3) covers 45% of the research area, which occupies the Northeast-Southeast part. The flow pattern (stream order) in this geomorphological unit is Trellis. Elevation 8-20º with an altitude of 112 to 200 mdpl, a flat slope of 6-25%, in the form of residual hilly land (Fig. 4). There is no developed structure. The lithology that composes this morphology is in the form of massive grey silt, clay with a parallel thin layer sediment structure, loose gravel sand, and fossil wood (Petrified Wood Stone). Exogenous processes in the form of weathering due to erosion by water, rubber plantations, oil palm plantations, and gold mining placer of the surrounding community.

c. Structural landform (horst) very steep geomorphological sub-unit

This unit has a Northwest-Southeast direction characterised by steep slopes (22-55%) with an elevation of 21-55º covering 25% of the study area. The geological structure found are wing anticline folds, minor folds, drag folds, and uphill faults. The dominant lithology is meta-sedimentary sandstone, slightly shale and shale insertion of sandstone, schist, and quartzite. This unit occupies Horst. In Fig. 3, there are two hills called Mudoh hills. Exogenous processes in the form of weathering due to erosion by water and illegal logging of natural forests cause landslides on every slope.

3.1.4 Flow pattern (stream order)

a. Trellis pattern

This flow pattern occupies an area of about 45% and develops in the Northeast-East and Southeast parts of the study area (Fig. 5). The structure of this unit is very influential on the pattern of river flow in the study area, characterising the hilly area next to the folds of the wing, rising faults, and joints. The river stages in this unit are generally mature stages with a U-shaped cross-section of the river (Fig. 5). The flow pattern develops in an area with sloping relief. The rock composition of the research area is in the form of massive grey silt, clay with parallel thin layer sediment structure, loose gravel sand, and wood fossils.

b. Sub-dendritic pattern

This flow pattern occupies an area of about 55% and develops in the southwest, west and northwest of the study area (see Fig. 5). Sub-dendritic is a modification of the dendritic flow pattern controlled very strongly by the hardness of the constituent rocks. This pattern has a rather steep to steep relief with the rock composition of the research area in the form of carbonated claystone, carbonated calcite, fine sandstone to coarse sandstone, conglomerate sandstone and coal weathering remnants act as fragments of very fine sandstone, as seen in Fig. 3a. The shape of the river body is associated with the charred river/point bar.

3.1.5 Structural geology analysis

a. Fault Analysis

Based on the geological structure data in the research area in the form of compression and tension joints and the rock layers' position, the relative stress direction is North, Northwest-South-Southeast. Based on these indications, the working structure in the study area is estimated to result from the transtension mechanism of the thrust fault found. This mechanism resulted in a lowland pattern in the research area. The transtension and fault mechanism manifestation is characterised by a thrust fault trending north-northwest and south-southeast resulting from the working force. This transtension mechanism results in a graben as a manifestation of the horst fault found in the study area. The spread of exposed shale units evidence this, and the results of age analysis show a difference in deposition time between sandstone units, so it is estimated that the sandstone units that are the Lower Member of Telisa Formation fill the lowlands.

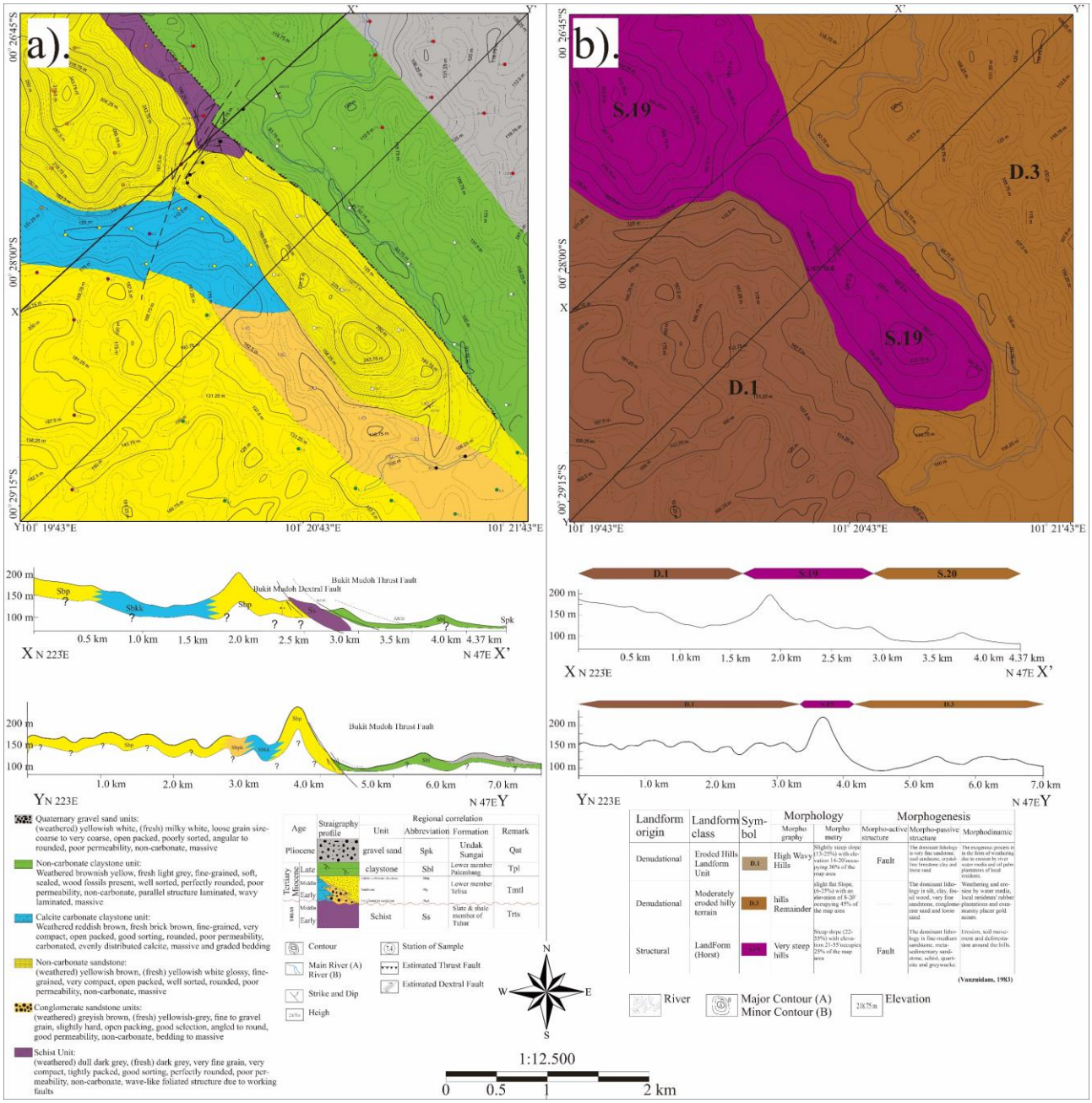

Fig. 3: a). Corrected Geological Map of Pulau Padang Village from the Field Validation (modified from Silitonga and Kastowo, 1975), b). Geomorphology map of Pulau Padang Village based on the field validation.

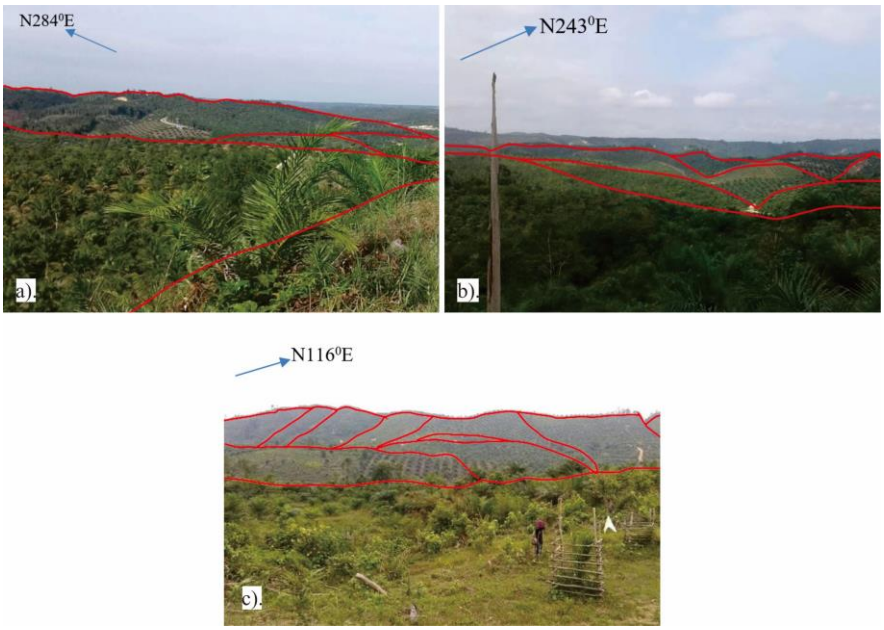

Fig. 4: Geomorphology Profile in Pulau Padang Village: a). Denudational of High Wavy Hills Geomorphological Sub-unit, b). Denudational of Remaining Hilly Landform Geomorphological Sub-Unit, c). Structural Landform (Horst) Very Steep Geomorphological Sub-Unit.

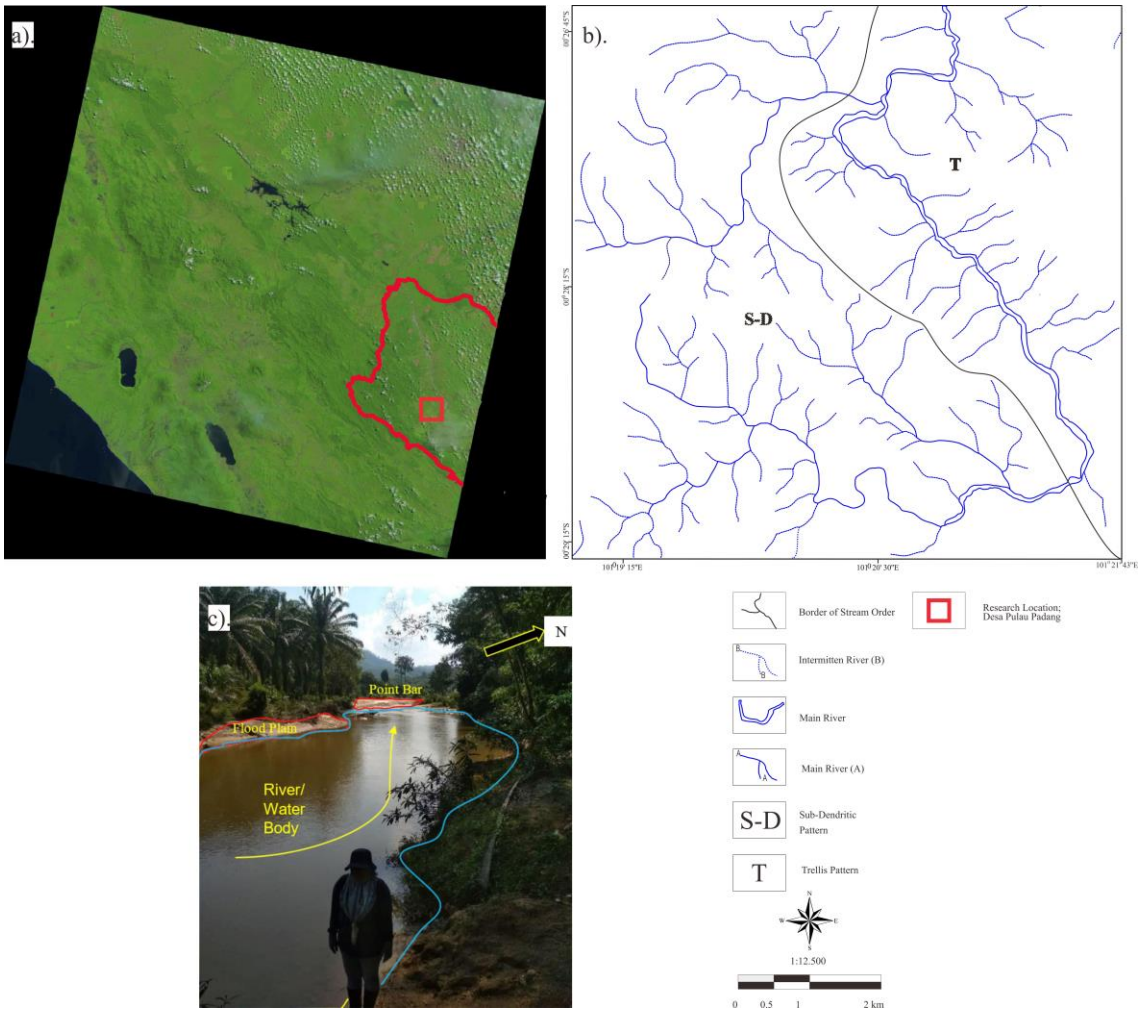

Fig. 5: a). Landsat 8 OLI/TIRS C2 L1 (Path 127 Row 60) Used in the Research Area (Red Box is Pulau Padang Village), b). Stream Order in Pulau Padang Village, c). The cross-section of the river with a "U" shape and width is ±18 m below the foot of Mudoh Hill. The photograph direction is N168^{0}E, with a layer of sandstone and a relatively strong current.

b. Joint analysis

Geological structures in the form of joints were identified in the study area. The joint data is processed using a stereonet to determine the direction of the main stress, which is very helpful in analysing the structural development in the research area. The following is a detailed explanation of each station with joint data (Table 2).

Table 2. Joint Measurement in Pulau Padang Village.

No.	St 7		St 15		St 22		St 40	
	Strike	Dip	Strike	Dip	Strike	Dip	Strike	Dip
1	306	84	150	86	200	54	200	54
2	295	86	140	82	25	38	25	38
3	300	80	158	67	356	12	356	12
4	314	81	245	84	271	75	271	75
5	315	64	240	76	294	48	294	48
6	315	65	325	49	214	63	142	26
7	306	82	332	36	354	46	354	46
8	307	90	14	76	271	66	271	66
9	263	87	335	55	89	83	89	83
10	310	83	340	21	353	35	353	35
11	268	89	210	16	279	44	279	44
12	266	76	335	83	12	51	12	51
13	205	90	325	89	290	64	290	64
14	280	89	25	76	285	44	285	44
15	302	86	320	90	165	16	235	16
16	330	60	340	89	35	34	35	34
17	325	75	20	86	271	70	271	70
18	315	55	332	76	79	73	79	73
19	300	65	15	74	26	55	26	55
20	320	45	340	86	75	70	75	70

Based on the joint calculation data analysis at station 7 (Fig. 6a) using the Dips application, the dominant stress direction is Southwest-Northeast, with the value of σ1 = 120º/90º. The measurement data for station 15 consists of 20 joint position data. The joint calculation identifies the dominant joint direction opposite each other. Fig. 6b shows the appearance of joints at station 15. Based on the joint calculation data results, it can be assumed that the dominant stress direction is Southwest to Northeast with a value of σ1 = 334º/90º. At station 22, the measurement data of this station consists of 20 joint data. The measurement of the joint was carried out by measuring the dominant direction of the paired joint. Based on the analysis of the joint data using the stereonet method (Dips application), it can be assumed that the direction of stress from the results of the joint calculation at the Southwest–Northeast trending location has a value of σ1 = 165º/79º. At station 40 (Fig. 6c), the measurement data for this station consists of 20 data on the joint position. The measurement of the joint was carried out by measuring the dominant direction in pairs. Based on the joint data analysis results, it can be assumed that the stress direction from the joint calculation results in the Southwest - Northeast trending location is σ1 = 275º/90º (see Fig. 6).

Lithological boundary drawing is done by identifying the visible characteristics of the image. Boundary drawing is based on hue, texture, shape, pattern, location, and their associations. Field observations and their correlation with the Landsat 8 imagery used can produce a complete geological map. The image also shows several lineament patterns, which can be interpreted as a developing geological structure pattern. After conducting a thorough analysis of the results of geological observations and measurements in the field and analysis of Landsat 8 satellite imagery, it is possible to produce a map of the geological structure that occurred in Pulau Padang Village, an area affected by the Great Sumatran Fault (Fig. 7).

3.2 Discussion

The subduction of the oceanic plate under the continental plate in the Sumatra area resulting The Great Sumatran Fault, which forms the Tertiary back-arc basin and knows as the Central Sumatra Basin, which contains economic hydrocarbon deposits. The study of the geological structure is primarily based on the interpretation of the satellite imagery used, complemented by field observations. In this research, the relationship between the deformation of horizontal (dextral) faults and the formation of large basins is known as pull-apart basins. The thrust fault was resulting from the dextral fault.

From the analysis of the satellite imagery and geological mapping in the field, it can be found that the mechanism for the formation of relatively small basins is in the horizontal and thrust fault deformation zones. Within this zone, there is movement between blocks that are convergent and divergent (see Fig. 3a, Fig. 6, and Fig. 7) and formed the highs and lows morphologies, respectively (Fig. 4). Based on the interpretation of satellite imagery and field validation, the rock unit distribution map refers to available geological maps, with factual modifications found in the field as seen in Fig. 3a and Fig. 7c.

On the edges of the Central Sumatra Basin, there are

many oil and gas deposits that are separated distribution. This situation was taken because the dextral fault activity by the Great Sumatran Fault occurred along the island of Sumatra. For the research area, this is proven by the finding of dextral fault structures, thrust fault, and joint structures, as shown in Fig. 3a, Fig. 6, and Fig. 7).

4. Conclusion

The research area of Pulau Padang Village is an area that contributes to the geological structure resulting from the formation of the Great Sumatran Fault. This area produced derived geological structures while the Great Sumatran Fault was formed. Field observations and making actual geological maps provide information related to the development of geological structures in this research area and are combined with satellite image analysis using Landsat 8 OLI/TIRS C2 L1 imagery, which is very supportive for making geological maps such as detailed lithological and geological structure information. Overall results, those analyses provide complete illustrations related to the formation and development of the Great Sumatran Fault in Pulau Padang Village.

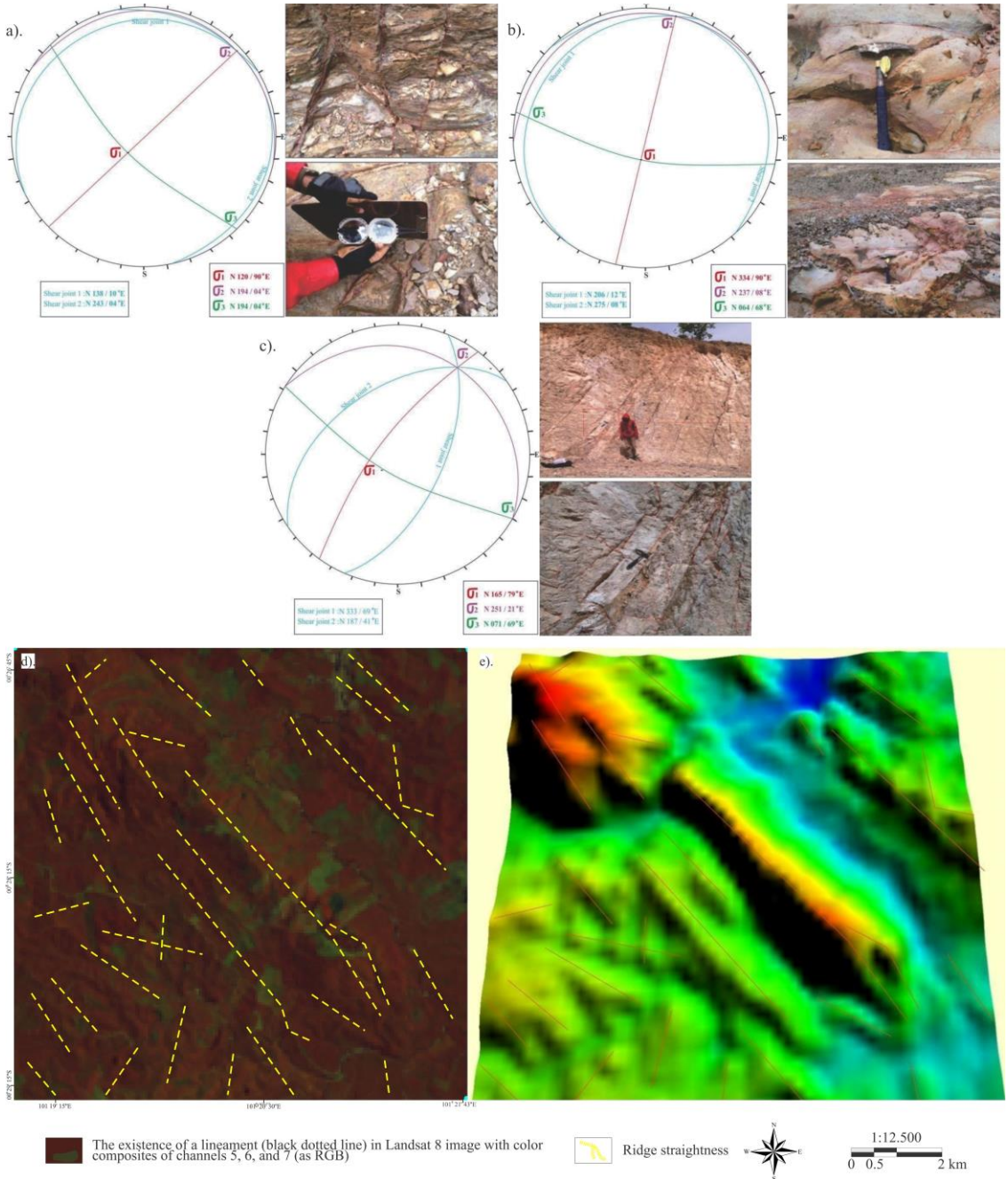

Fig. 6: Joint Measurement Analysis in Pulau Padang Village: a). Station 7, b). Station 15, c). Station 40, Ridge Straightness Pattern in Pulau Padang Village: d). Lineament Extraction from Field Measurement to Corrected Landsat 8 Image, e). Comparison to the Digital Elevation Model in the Research Area.

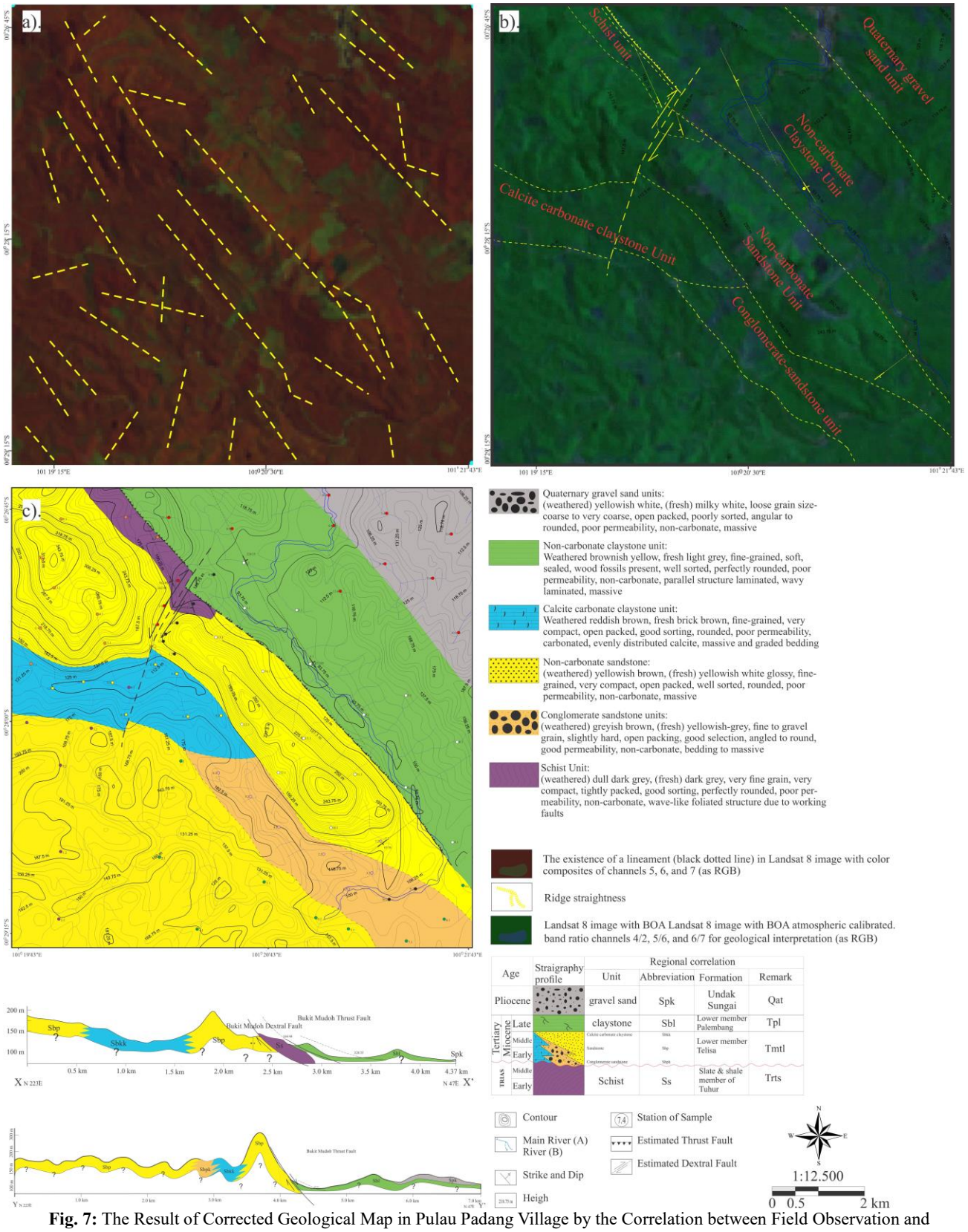

Fig. 7: The Result of Corrected Geological Map in Pulau Padang Village by the Correlation between Field Observation and Validation with Landsat 8 Analysis: a). Map of Lineament Distribution of Pulau Padang Village, b). Map of Structural Distribution of Pulau Padang Village, c). Corrected Geological Map of Pulau Padang Village.

Acknowledgements

The authors thank all who supported this research activity, especially the Government of Kuantan Singingi Regency and the Government of Riau Province, for supporting the provision of secondary data. Furthermore, the authors would like to thank Universitas Islam Riau, Chiba University, Japan, Politeknik Batam, who continue to support the research collaborations, especially the Geological Engineering Program, Universitas Islam Riau, Center for Environmental Remote Sensing, Chiba University, Japan, and Department of Geomatics Engineering, Politeknik Negeri Batam.

References

1) Sahara, David P., Sri Widiyantoro, and Masyhur Irsyam. "Stress heterogeneity and its impact on seismicity pattern along the equatorial bifurcation zone of the Great Sumatran Fault, Indonesia." *Journal of Asian Earth Sciences* 164 (2018): 1-8. https://doi.org/10.1016/j.jseaes.2018.06.002.
2) Bening, Maulidia A., et al. "Modeling the Impact of the Viscoelastic Layer Thickness and the Frictional Strength to the Lithosphere Deformation in a Strike-Slip Fault: Insight to the Seismicity Pattern along the Great Sumatran Fault." *GeoHazards* 3.4 (2022): 452-464. https://doi.org/10.3390/geohazards3040023
3) Hady, Aulia Kurnia, and Gayatri Indah Marliyani. "Updated Segmentation Model of the Aceh Segment of the Great Sumatran Fault System in Northern Sumatra, Indonesia." *Journal of Applied Geology* 5.2 (2020): 84-100. http://dx.doi.org/10.22146/jag.56134
4) Mutebi, Denis, et al. "Variation of Rock Electrical Resistivity in Andesitic-Trachytic Volcanic Geothermal Areas. A Case Study of Lili-Sepporaki, Sulawesi island-Indonesia." *Evergreen*, 7(3) 314-322 (2020). https://doi.org/10.5109/4068609
5) Qiu, Qiang, and Chung-Han Chan. "Coulomb stress perturbation after great earthquakes in the Sumatran subduction zone: Potential impacts in the surrounding region." *Journal of Asian Earth Sciences* 180 (2019): 103869. https://doi.org/10.1016/j.jseaes.2019.103869
6) Rivai, Tomy Alvin, Kotaro Yonezu, and Koichiro Watanabe. "Mineralogy and geochemistry of host rocks and orebodies at the anjing hitam prospect (Dairi, north sumatra, indonesia) and their environmental implications." *Evergreen,* 6(1) 18-28. (2019): https://doi.org/10.5109/2320997
7) Natawidjaja, Danny H. "Updating active fault maps and sliprates along the Sumatran Fault Zone, Indonesia." *IOP Conference Series: Earth and Environmental Science*. Vol. 118. No. 1. IOP Publishing, 2018. https://doi.org/10.1088/1755-1315/118/1/012001
8) Ritonga, Magdalena, and Tobi Prayoga. "Identification of Mengkarang Isoclinal Folds Against the Effect of Sumatran Fault Force in Air Batu Village and Surrounding Merangin Jambi Geopark." *Jurnal IPTEK* 26.1 (2022): 51-58. https://doi.org/10.31284/j.iptek.2022.v26i1.2999
9) Daryono, Sapto Kis, et al. "Facies and architectural analysis of Paleogen fluvial deposits of the measured section of Rambangnia and Air Napalan Rivers in Palembang Sub-basin." *Journal of Earth and Marine Technology (JEMT)* 3.1 (2022): 24-33. https://doi.org/10.31284/j.jemt.2022.v3i1.3606
10) Kausarian, H., et al. "Geochemical Analysis of Metal Minerals on Kuantan Singingi Regency, Riau Province as a Connection part of Bukit Barisan Mountain, West Sumatera, Indonesia." *International Journal on Advanced Science, Engineering And Information Technology* 11.2 (2021): 682-689. DOI:10.18517/ijaseit.11.2.11960
11) Prawirodirdjo, Linette, and Yehuda Bock. "Instantaneous global plate motion model from 12 years of continuous GPS observations." *Journal of Geophysical Research: Solid Earth* 109.B8 (2004). https://doi.org/10.1029/2003JB002944
12) Syukri, Muhammad, et al. "Spatial and Temporal Analysis of b-value Imaging Characteristics Using High Precision Earthquake Spot in the Sumatran Subduction Zone." *The Iraqi Geological Journal* (2021): 1-11. https://doi.org/10.46717/igj.54.2B.1Ms-2021-08-21
13) Alif, Satrio Muhammad, and Arliandy Pratama. "Analysis of southern segment of Sumatran Fault monitoring bench mark as preliminary approach in updating earthquake hazard map." *Journal of Science and Applicative Technology* 2.1 (2019): 183-191. https://doi.org/10.35472/281470
14) Sonny Abfertiawan, M., et al. "Hydrology Simulation of Ukud River in Lati Coal Mine." *Evergreen: joint journal of Novel Carbon Resource Sciences & Green Asia Strategy,* 3(1) 21-31 (2016). https://doi.org/10.5109/1657737
15) Dimyati, Ratih Dewanti, Projo Danoedoro, and Muhammad Dimyati. "Digital interpretability of annual tile-based mosaic of landsat-8 OLI for time-series land cover analysis in the Central Part of Sumatra." *Indonesian Journal of Geography* 50.2 (2018): 168-183. https://doi.org/10.22146/ijg.35046
16) Ghadamode, Vikas, et al. "Spatial analysis techniques for tsunami vulnerability and inundation mapping of Andaman region using remote sensing, GIS, AHP, and Fuzzy logic methods." *Environmental Earth Sciences* 81.17 (2022): 1-18. https://doi.org/10.1007/s12665-022-10548-w
17) Mertosono, Suwahjuhadi, and G. A. S. Nayoan. "The Tertiary basinal area of central Sumatra." (1974): 63-76.
18) Tusara, Loren, and Ryuichi Itoi. "Characterization of

Solid Deposits formed in Geothermal Surface Facilities." *Evergreen,* 1(1) 6-13 (2014). https://doi.org/10.5109/1440969

19) Fardiansyah, Iqbal, Agung Wiyono, and Abdullah Faisal Talib. "The Massive Fluvial Channel System in The Balam Graben: New Insight and Future Expectation from Menggala Formation in The Northern Rokan Block, Central Sumatera Basin." *Indonesian Association of Geologists Journal (IAGI Journal)* 1.2 (2021): 103-110. http://doi.org/10.51835/iagij.2021.1.2.34
20) Dwiki, Sendy. "Development of Environmental Policy in Indonesia regarding Mining Industry in Comparison with the United States and Australia: The Lesson That Can Be Learned." *Evergreen* , 5(2) 50-57 (2018). https://doi.org/10.5109/1936217
21) Muslihudin, Muslihudin, et al. "Environmental Constraints in Building Process a Sustainable Geothermal Power Plant on The Slopes of Slamet Mount, Central Java, Indonesia." *Evergreen,* 9(2) 300-309 (2022). https://doi.org/10.5109/4793669
22) Heidrick, Tom L., and Karsani Aulia. "A structural and tectonic model of the coastal plains block, Central Sumatra Basin, Indonesia." (1993): 285-317. https://doi.org/10.29118/IPA.572.285.317
23) Muljana, Budi, Koichiro Watanabe, and Mega F. Rosana. "Source-rock Potential of the Middle to Late Miocene Turbidite in Majalengka Sub-basin, West Java Indonesia: Related to Magmatism and Tectonism." *Journal of Novel Carbon Resource Sciences* 6 (2012): 15-23.
24) Prayitno, Budi, and Susilo Susilo. "Geology Of Tanjung Medan, Rokan IV Koto, Rokan Hulu District, Riau Province." *Journal of Geoscience, Engineering, Environment, and Technology* 3.2 (2018): 123-127. https://doi.org/10.24273/jgeet.2018.3.2.1597
25) Maryati, Sri, et al. "Determine Appropriate Post Mining Land Use in Indonesia Coal Mining Using Land Suitability Evaluation." *Journal of Novel Carbon Resource Sciences* 5 (2012): 33-38.
26) Katili, John A. "A review of the geotectonic theories and tectonic maps of Indonesia." *Earth-Science Reviews* 7.3 (1971): 143-163. https://doi.org/10.1016/0012-8252(71)90006-7
27) Koesoemadinata, R. P., and Th Matasak. "Stratigraphy and Sedimentation: Ombilin Basin, Central Sumatra (West Sumatra Province)." (1981): 217-249.
28) Prayitno, B., Riva'i, M., Suryadi, A., Kausarian, H., Rozi, F. "Analysis of Stratigraphy and Sedimentation Dynamics of Coal, Sawahlunto Formation, Ombilin Basin." *Geomate Journal* 17.63 (2019): 255-262. https://doi.org/10.21660/2019.63.ICEE24
29) Patria, Aulia Agus, and Ferian Anggara. "Microfacies and Depositional Environment of the Eocene Sawahlunto Coal, Ombilin Basin, Indonesia." *The Iraqi Geological Journal* (2022): 127-145. https://doi.org/10.46717/igj.55.1E.11Ms-2022-05-27
30) Roy, Sandip Kumar. "Middle and Lower Eocene Coals, Cambay Basin and Miocene Coals, South Sumatra Basin: Analogs for Coal and CBM Properties." *SPE Oil and Gas India Conference and Exhibition*. OnePetro, 2019. https://doi.org/10.2118/194651-MS
31) Haris, Abdul. "Integrated Geological and Geophysical Approach to Reservoir Modeling: Case Study of Jambi Sub-basin, Sumatra, Indonesia." *Journal of the Geological Society of India* 95.2 (2020): 197-204. . https://doi.org/10.1007/s12594-020-1410-7
32) Julikah, Julikah, Ginanjar Rahmat, and Muhammad Budisatya Wiranatanegara. "Subsurface Geological Evaluation of the Central Sumatra Basin in Relation to the Presence of Heavy Oil." *Scientific Contributions Oil and Gas* 44.1 (2021): 65-81. https://doi.org/10.29017/SCOG.44.1.491
33) Syamsuddin, E., K. Shehzad, and S. Wahyuni. "Bio-markers based oil to source rock correlation and paleo-environmental interpretation: A case study from Talang Akar Formation, South Sumatra Basin, Indonesia." *Journal of Physics: Conference Series*. Vol. 1341. No. 8. IOP Publishing, 2019. https://doi.org/10.1088/1742-6596/1341/8/082023
34) Signorelli, Javier H., and JGM Han Raven. "Current knowledge of the family Cardiliidae (Bivalvia, Mactroidea)." *Journal of Paleontology* 92.2 (2018): 130-145. https://doi.org/10.1017/jpa.2017.86
35) Yanis, Muhammad, Marwan Marwan, and Nazli Ismail. "Efficient Use of Satellite Gravity Anomalies for mapping the Great Sumatran Fault in Aceh Province." *Indonesian Journal of Applied Physics* 9.02 (2019): 61-67. https://doi.org/10.13057/ijap.v9i2.34479
36) Gerace, Aaron, et al. "Towards an operational, split window-derived surface temperature product for the thermal infrared sensors onboard Landsat 8 and 9." *Remote Sensing* 12.2 (2020): 224. https://doi.org/10.3390/rs12020224
37) Bahar, Hendra, and Muhammad Taufik. "Remote Sensing Analysis Using Landsat 8 Data For Lithological Mapping-A Case Study In Mount Penanggungan, East Java, Indonesia." *IPTEK Journal of Proceedings Series* 3.2 (2017): 90-92. http://dx.doi.org/10.12962/j23546026.y2017i2.2303
38) Adiri, Zakaria, et al. "Lithological mapping using Landsat 8 OLI and Terra ASTER multispectral data in the Bas Drâa inlier, Moroccan Anti Atlas." *Journal of Applied Remote Sensing* 10.1 (2016): 016005. https://doi.org/10.1117/1.JRS.10.016005
39) Vermote, E. F. T. D., et al. "Second simulation of a satellite signal in the solar spectrum-vector (6SV)." *6S User Guide Version* 3.2 (2006): 1-55. 10.1109/36.581987
40) Van Zuidam, Robert Antonius. *Terrain analysis and*

classification using aerial photographs: a geomorphological approach. No. 526.982 V3. 1979.